




Mutational meltdown of putative microbial altruists in *Streptomyces coelicolor* colonies

Zheren Zhang ^{1,3}✉, Shraddha Shitut^{1,2}, Bart Claushuis ¹, Dennis Claessen^{1,4} & Daniel E. Rozen ^{1,4}✉

In colonies of the filamentous multicellular bacterium *Streptomyces coelicolor*, a subpopulation of cells arises that hyperproduces metabolically costly antibiotics, resulting in a division of labor that increases colony fitness. Because these cells contain large genomic deletions that cause massive reductions to individual fitness, their behavior is similar to altruistic worker castes in social insects or somatic cells in multicellular organisms. To understand these mutant cells' reproductive and genomic fate after their emergence, we use experimental evolution by serially transferring populations via spore-to-spore transfer for 25 cycles, reflective of the natural mode of bottlenecked transmission for these spore-forming bacteria. We show that in contrast to wild-type cells, putatively altruistic mutant cells continue to decline in fitness during transfer while they lose more fragments from their chromosome ends. In addition, the base-substitution rate in mutants increases roughly 10-fold, possibly due to mutations in genes for DNA replication and repair. Ecological damage, caused by reduced sporulation, coupled with DNA damage due to point mutations and deletions, leads to an inevitable and irreversible type of mutational meltdown in these cells. Taken together, these results suggest the cells arising in the *S. coelicolor* division of labor are analogous to altruistic reproductively sterile castes of social insects.

¹Institute of Biology, Leiden University, Sylviusweg 72, 2333 BE Leiden, the Netherlands. ²Origins Center, Nijenborgh 7, 9747 AG Groningen, the Netherlands. ³Present address: Department of Zoology, University of Oxford, 11a Mansfield Road, Oxford OX1 3SZ, UK. ⁴These authors jointly supervised this work: Dennis Claessen, Daniel E. Rozen. ✉email: zheren.zhang@zoo.ox.ac.uk; d.e.rozen@biology.leidenuniv.nl

Multicellular organisms show enormous variation in size and complexity, ranging from multicellular microbes to sequoias and whales, and from transient undifferentiated cellular clusters to stable individuals with highly specialized cell types. Despite their differences, a recent study showed that a central factor determining organismal complexity is the way in which multicellular organisms are formed¹. Clonal groups, where relatedness among cells is high, show more cellular specialization and an increased likelihood of expressing the reproductive division of labor between somatic and germ cells^{1–4}. By contrast, groups with aggregative multicellularity like dictyostelid social amoebae or myxobacteria, which potentially have lower relatedness between cells if unrelated genotypes coaggregate during development, tend to show reduced specialization^{5–7}. Thus, in analogy with sterile castes of workers within colonies of social insects that are morphologically differentiated to perform specialized tasks, the extreme altruism needed for reproductive sterility is facilitated by high relatedness⁸.

In microbes, the requirement of high relatedness is most easily met if colonies are initiated from a single cell or spore. High relatedness during multicellular growth or development is even further guaranteed if the cells within colonies remain physically connected to each other, as observed in filamentous streptomycetes^{9,10}. These bacteria have a well-characterized reproductive division of labor due to a developmental program that leads to the formation of durable spores following a period of vegetative growth and the elongation of spore-bearing aerial hyphae^{11,12}. In addition, we have recently shown that colonies are further divided into a subpopulation of cells that hyperproduces antibiotics¹³. The ability to generate this subpopulation of cells appears to benefit the whole colony, by virtue of their increased antibiotic production, without causing a decline in overall colony spore production. However, the fitness of the mutant subpopulation is significantly reduced. Here we provide a detailed examination of the evolutionary fate of these specialized cells and provide evidence that they represent a terminally differentiated putatively altruistic cell type within these multicellular microbes.

Streptomyces are bacteria that live in the soil and produce a broad diversity of antibacterial and antifungal compounds, among other specialized metabolites^{14,15}. Division of labor allows *Streptomyces coelicolor* colonies to partly offset the metabolic cost of producing these compounds¹³. However, differentiation into this hyperproducing cell type is accompanied by huge fitness costs due to massive deletions of up to 1 Mb at the ends of their linear chromosomes. Examining independent mutant strains, we have found a strong positive correlation between the size of genomic deletions and the amount of antibiotics produced, as well as a strong negative correlation between the deletion size and spore production. In addition, as shown earlier¹³ and in Fig. 1a, competition assays revealed that mutant strains were strongly disadvantaged. Indeed, even when the initial frequency of mutants in mixed colonies was as high as ~80%, their final frequency declined to less than 1% after one cycle of colony growth. These results indicated that mutant strains would be quickly eliminated during competitive growth. We hypothesized that, like sterile insect workers or somatic cells that are differentiated to perform specialized tasks, these putatively altruistic cells represent a sterile microbial caste because they are functionally cohesive, showing uniformly increased antibiotic production, and arise due to a shared mechanism of genome deletions. However, as our results were based on static colonies, we lacked insight into the fate of these cells after they emerged.

To address this question, the current study tracks the fate and fitness of mutant and wild-type (WT) lineages during short-term experimental evolution. To reflect the manner of spore-to-spore reproduction in these bacteria, lineages were serially transferred

via single colonies using a mutation accumulation (MA) design¹⁶ (Fig. 1b). In contrast to much longer-term experiments using this approach in other microbes, where fitness declines extremely slowly^{17,18}, we observed significant fitness reductions, including extinction, in our mutant lineages after only 25 transfers. These changes were not only associated with continued deletions at the chromosome ends but also the tendency for lineages to become hypermutators likely due to errors in genes for DNA replication and repair^{19,20}. Together these data support the idea that this specialized subpopulation of cells within *Streptomyces* colonies is analogous to a functionally differentiated sterile caste that persists due to their inclusive fitness benefits to the entire colony and further highlight the idea that clonal propagation and high relatedness can give rise to a broad diversity of functionally specialized cells within these multicellular bacteria.

Results

Phenotypic changes during serial transfer. To track the fate of different mutant lineages harboring different spontaneous genomic deletions we transferred six wild types (WTs) (W1–W6) and six mutants (M1–M6) for 25 transfers using a MA design¹⁶ through single spore bottlenecks twice per week (Fig. 1b). Details of strain origins are given in Methods. Consistent with our earlier results¹³, we first confirmed that the starting competitive fitness of a subset of these mutants was significantly reduced compared to the WT ancestor (Fig. 1a). Even when mutant lineages were inoculated at an initial frequency as high as roughly 80%, their final frequency during pairwise competition declined to less than 1%. In addition, the mutant strains that were used to initiate the MA experiment produced significantly fewer colony-forming units (CFUs) after clonal development than their WT counterparts (Wilcoxon rank sum test, $P=0.002$, see below). Strains were sampled approximately every five transfers, with the exception of one WT lineage (W3) that was sampled more frequently after it acquired chromosome deletions after the 7th transfer (see below). One of the six mutant lineages (M2) acquired a bald morphology after the 5th transfer and became functionally extinct due to a total loss of spore production and was not included in fitness and antibiotic production analyses (Supplementary Fig. 1).

To identify phenotypic changes in evolved lineages, we screened for two easily scorable traits that are indicative of deletions to the right chromosome arm¹³. Chloramphenicol susceptibility, due to the loss of *cmr1* (SCO7526) and *cmr2* (SCO7662), indicates a deletion of at least 322 kb^{21,22} and arginine auxotrophy, due to the loss of *argG* (SCO7036), corresponds to a deletion of at least 843 kb²³. In addition, we analyzed changes to resistance to three other antibiotics. As is evident in Fig. 2a, whereas the WT lineages remained resistant to chloramphenicol (except for W3), the minimal inhibitory concentration (MIC) of mutant lineages was lower than the WT lineages and declined during the course of the experiment. On the basis of these results, W3 was hereafter analyzed as a mutant lineage despite its WT origin. A trend towards increased arginine auxotrophy was also observed in mutant lineages (Fig. 2b), suggesting that continuous chromosome deletions occurred during the course of the experiment (genomic changes are described below). Tests for susceptibility to other antibiotics (Supplementary Fig. 2) also showed similar trends as those found for chloramphenicol, with the exception of the bald populations from M2 that showed a four-fold increase in the MIC for ciprofloxacin.

Fitness and antibiotic production in evolved lineages. Figure 3a shows that the CFU of mutant lineages declined continuously

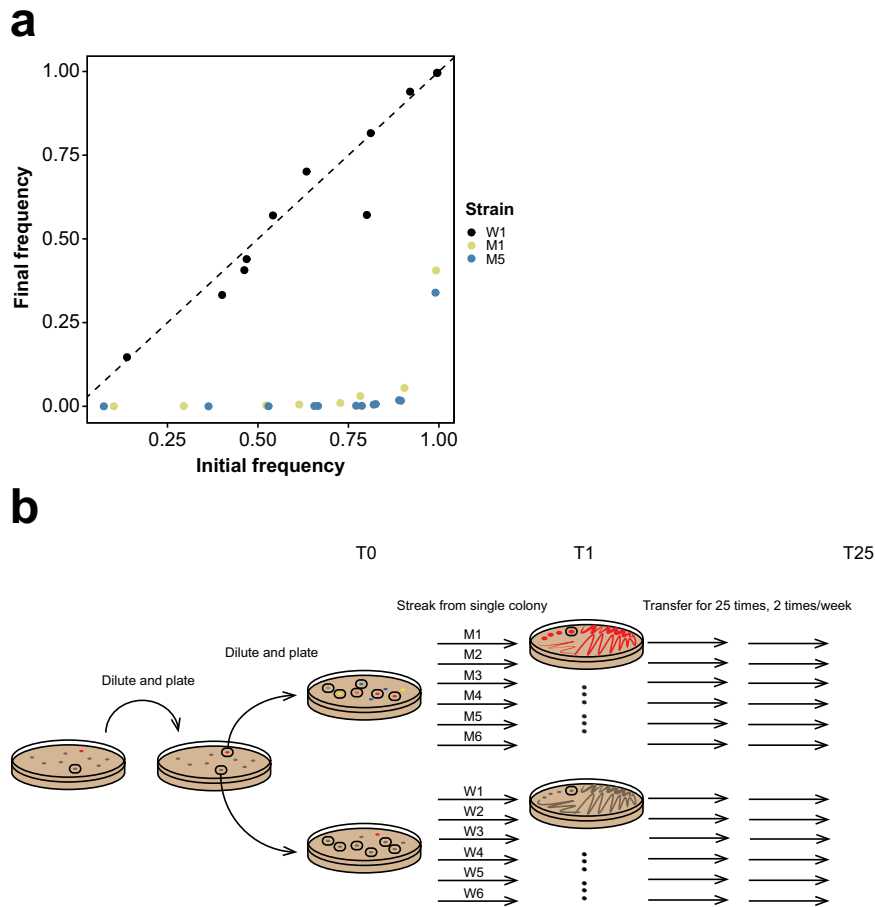


Fig. 1 Overview of the experimental design. **a** Initial and final frequency of three T0 strains from different lineages during the 5-day competition with the WT ancestor. The dashed line shows the expectation if initial and final frequencies are equal, as seen for the strain from the WT lineage (W1). By contrast, mutant fitness (M1 and M5) is dramatically lower than the WT, dropping to <1% even when starting from as high as approximately 73% (M1) or 83% (M5). **b** The schematic of our experimental setup. An ancestral WT colony was picked and plated to obtain individual colonies. One mutant and one WT colony were picked and plated to obtain six WT and six mutants clones. Lineages were subsequently transferred via single colony bottlenecks for 25 transfers. During each transfer the colonies were randomly-chosen and each time point of these transfers is designated as T plus the transfer number.

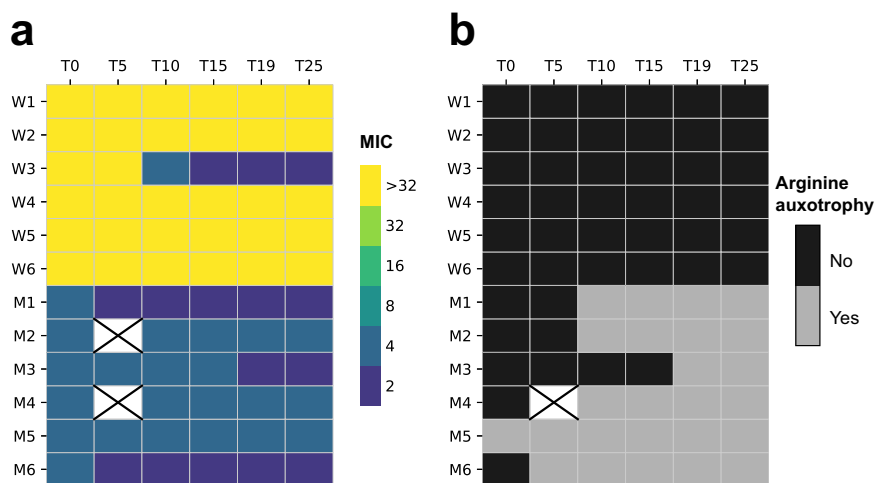


Fig. 2 Phenotypic results for transferred lineages based on two genetic markers in the right chromosome arm. **a** MIC ($\mu\text{g ml}^{-1}$) of chloramphenicol over time. **b** Arginine auxotrophy over time.

compared to WT lineages. M2, which went extinct after the 5th transfer, was only evaluated for the first two time points, and W3 was treated as a mutant lineage from the 7th transfer, as explained above. Of the mutant lineages, all seven showed significant

reductions in CFU during the experiment (Welch’s *t* test, all $P < 0.01$), amounting to a 9.8-fold median decline (interquartile range [IQR] 5.4–13.3; one-sample Wilcoxon signed rank test, $P = 0.016$). By contrast, four of six WT lineages showed small but

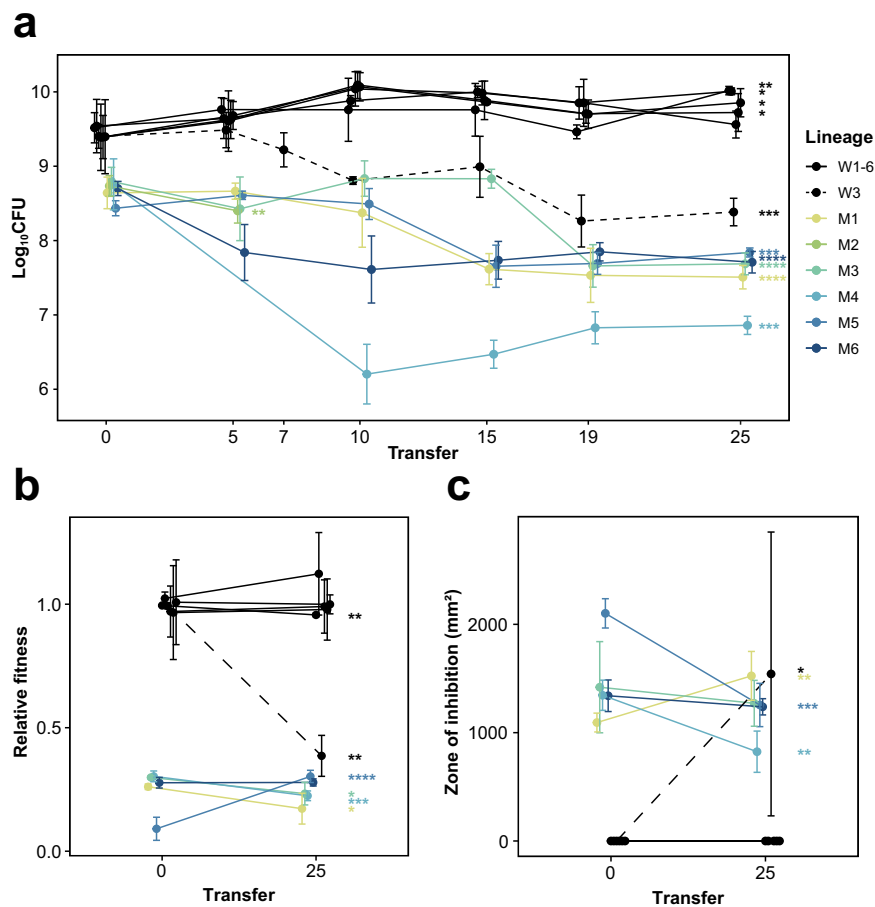


Fig. 3 Fitness and antibiotic production in evolved lineages. **a** The fitness in terms of CFU of each lineage through time. WT lineages are shown in black with the one lineage W3 distinguished by a dashed line to indicate a conversion to mutant form after the 7th transfer. The mutant lineages all show an overall decline through time with one lineage, M2, completely dying after the 5th transfer. **b** Relative fitness of ancestor and evolved strains during competition with the WT. WT lineages show no significant change over time except for W1 and W3. The evolved strains in the mutant lineages show an overall decline in relative fitness except for M5. **c** Antibiotic production measured as the zone of inhibition for the ancestor and evolved strains of all lineages. WT lineages except for W3 show no change in antibiotic production. Mutant lineages show significant differences in antibiotic production. Dots and error bars represent means and 95% confidence intervals calculated from $n = 2-4$ biologically independent replicates (details are given in Methods). Levels of statistical significance are indicated as $*P < 0.05$, $**P < 0.01$, $***P < 0.001$, and $****P < 0.0001$ (Welch's t test or one-sample t test).

significant, increases in CFU (Welch's t test, all $P < 0.05$), amounting to a 2.4-fold median fitness increase (IQR 1.6–2.8; one-sample Wilcoxon signed rank test, $P = 0.031$). Accordingly, as shown in Supplementary Fig. 3, the median CFU change of WT and mutant lineages were significantly different from each other (Wilcoxon rank sum test, $P = 0.0012$).

To further examine changes during the MA, the relative fitness of all ancestral and evolved strains was measured using a pairwise competition assay. Results in Fig. 3b are consistent with those based on CFU, and the two fitness measures were significantly correlated (Pearson's product-moment correlation, $r = 0.866$, $df = 20$, $P = 1.928 \times 10^{-7}$) (Supplementary Fig. 4). Except for W1 and W3, the fitness of WT lineages remained unchanged, while most mutant lineages had significantly reduced fitness (Welch's t test, all $P < 0.05$). The fitness of one lineage (M5) surprisingly increased from its initial value, suggesting that CFU, which measures the sporulation rate, may also be impacted by other aspects of *Streptomyces* multicellular growth that are important during fitness assays.

Finally, we estimated antibiotic production of evolved lineages using an overlay assay (Fig. 3c). As expected, mutant strains produced significantly larger zones of inhibition than WT strains at the start (Wilcoxon rank sum test with continuity correction,

$P = 0.004$) and the end (Wilcoxon rank sum test with continuity correction, $P = 0.005$) of the serial transfer. While WT lineages remained unchanged and produced small zones of inhibition against the *Bacillus subtilis* target species, average antibiotic production in all mutant lineages remained extremely high, while three lineages showed small but significant (Welch's t test, all $P < 0.01$). Notably, antibiotic production in W3 increased markedly, coincident with its decreased fitness; this change confirms the strong correlation between the two traits¹³.

Continuous deletions in mutant lineages but not WT lineages.

To identify genetic changes that led to the rapid declines in mutant CFU, we used whole-genome sequencing to measure changes in genome size by mapping against a reference strain (Supplementary Fig. 5). As expected, no changes were observed in WT lineages (with the exception of W3 from the 7th transfer). By contrast, as shown in Fig. 4a and Supplementary Fig. 5, mutant lineages continued to accumulate large deletions to the left and right chromosome arms during serial transfer. Deletions in the left arm ranged from 0 to 882 kb, and in the right arm from 0 to 250 kb (Left arm: 289 kb (mean), $n = 7$; Right arm: 80 kb (mean), $n = 7$). The total deletion size of these strains ranged from 0 to 924 kb (369 kb (mean), $n = 7$). One lineage (M2) suffered a large

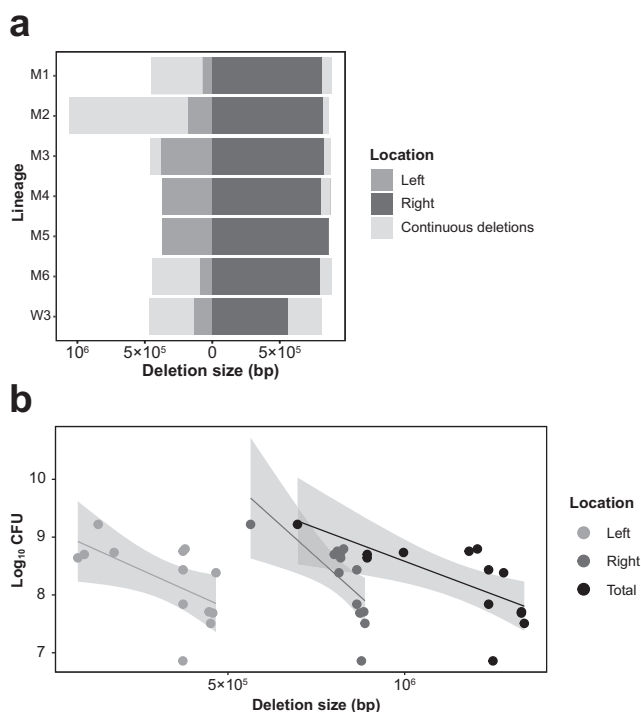


Fig. 4 Genomic deletions and their effects on strain fitness. **a** Initial and final deletion sizes in the left and right chromosome arms. Dark gray regions represent deletions in the left and right chromosome arms of ancestral strains, while regions in light gray represent new deletions in evolved strains. Sequenced strains include M1-M6 and W3 at T0 (or T5 for W3) and T25. **b** Significant negative correlation between the size of the genomic deletions and strain fitness, shown for the left arm, the right arm and the entire genome. Linear regression lines include 95% confidence intervals. Statistics are given in the main text.

deletion in the left chromosome arm, and this strain was no longer able to develop an aerial mycelium, resulting in a bald phenotype (Supplementary Fig. 1). However, no apparent deletions in known *bld* genes could be identified²⁴, suggesting other causes for this phenotype. Additionally, one lineage (M5) that began with the shortest genome did not gain further deletions, suggesting that further genome loss may not have been possible due the presence of essential genes near the border of the chromosome ends. Intriguingly, this is also the only mutant lineage in which we observed an increased relative fitness during the MA experiment (Fig. 3b), suggesting that changes to this strain were due to point mutations. Figure 4b plots the relationship between the CFU and the size of genomic deletions in the left arm, the right arm, or the entire chromosome. These results confirm and extend our previous observations that the CFU and the deletion size are negatively correlated for the left arm (Pearson's product-moment correlation, $r = -0.595$, $df = 11$, $P = 0.032$), the right arm ($r = -0.688$, $df = 11$, $P = 0.009$), and for the whole chromosome ($r = -0.703$, $df = 11$, $P = 0.007$).

Increased base-substitution rates in mutant lineages. To address other sources of mutational variation, in addition to gross chromosome changes, we estimated the base-substitution and indel mutation rates from mutant and WT lineages. Unexpectedly, we found that mutant lineages fixed significantly more mutations than the WT lineages. Overall, mutants fixed 29.5 mutations per lineage (median, IQR 12.25–32.5, $n = 6$) while the WT lineages fixed five mutations per lineage (median, IQR 4–6, $n = 5$). To account for differences in the number of transfers of

different lineages (due to the impact of W3 that became a mutant after the 7th transfer), we calculated a per transfer mutation rate. This analysis showed that the base-substitution rate for mutants was 12.78 per 10^8 nucleotides per transfer (median, IQR 7.62–17.46, $n = 7$) compared to 1.5 per 10^8 nucleotides per transfer (median, IQR 1.28–2.03, $n = 6$) in WT, exhibiting a roughly 10-fold difference (Wilcoxon rank sum test with continuity correction, $U = 4$, $P = 0.018$) (Fig. 5a). When we partitioned this result into different mutant classes, we observed that mutants acquired synonymous and non-synonymous mutations as well as changes in non-coding regions at a significantly higher rate (Fig. 5b). Further, looking across different transitions and transversions, we found that mutants fixed more mutations in four out of six mutation classes (Fig. 5c). Four mutant lineages fixed mutations in alleles affecting DNA replication or repair^{19,20}, including DNA polymerase III (synonymous), DNA topoisomerase IV (synonymous), DNA polymerase I (non-synonymous), and DNA ligase (non-synonymous) (Supplementary Data 1). Although suggestive, at present we cannot confirm that these specific changes are causally associated with increased mutation fixation.

Our results thus indicate that mutant lineages become mutators, in addition to acquiring large genomic deletions. Both factors likely contribute to their dramatic fitness reductions.

Discussion

Division of labor allows populations of individuals to more efficiently carry out functions that are mutually incompatible^{3,25,26}. In microbes, division of labor can facilitate biofilm formation^{25,27}, energy transfer²⁸, and coordinated metabolism²⁹, among other behaviors. In some cases, division of labor leads to subpopulations of cells that carry out functions that are lethal to themselves but that benefit the entire colony³⁰. For example, colicin secretion in *Escherichia coli* requires cell lysis³¹, a fate limited to a small fraction of cells with low reproductive value. By this process, the burden of colicin secretion is disproportionately borne by the cells with the least to lose in terms of their own fitness^{32,33}. We recently provided evidence for a similar phenomenon in *Streptomyces*, whereby a subfraction of cells within a multicellular colony hyperproduces antibiotics at the expense of their own reproduction, in part due to large and irreversible deletions from their chromosome ends¹³. The aim of the present study was to examine the fate of these cells after their emergence. We found that although *Streptomyces* cells hyperproducing antibiotics do not lyse, like *E. coli* colicin producers, they continue to accumulate large deletions and also evolve an increased mutation rate across their genome. These effects, which lead to an “effective lethality”, suggest that these cells are analogous to the reproductively sterile worker castes in social insects³⁴.

Our experimental approach was designed to approximate the natural growth and development of *Streptomyces* that disperse via spores, such that each new colony passes through a single cell bottleneck. This resembled a classic MA experimental design, which has been widely used to examine fitness declines in microbes due to the accumulation of deleterious mutations via Muller's ratchet, a process in which deleterious mutations accumulate irreversibly in a population lacking recombination^{35,36}. As in MA experiments, our mutants lost fitness^{17,18}; however, their rate of decline was more rapid due to mutations of very large effects via genome loss as well as point mutations. Results in Fig. 4b show a significant negative relationship between the total genome loss and CFU production, consistent with studies performed in *E. coli* containing manipulated reduced genomes³⁷. Given the 679–1817 genes that are lost from these populations, it is not possible to know which ones are responsible for the fitness

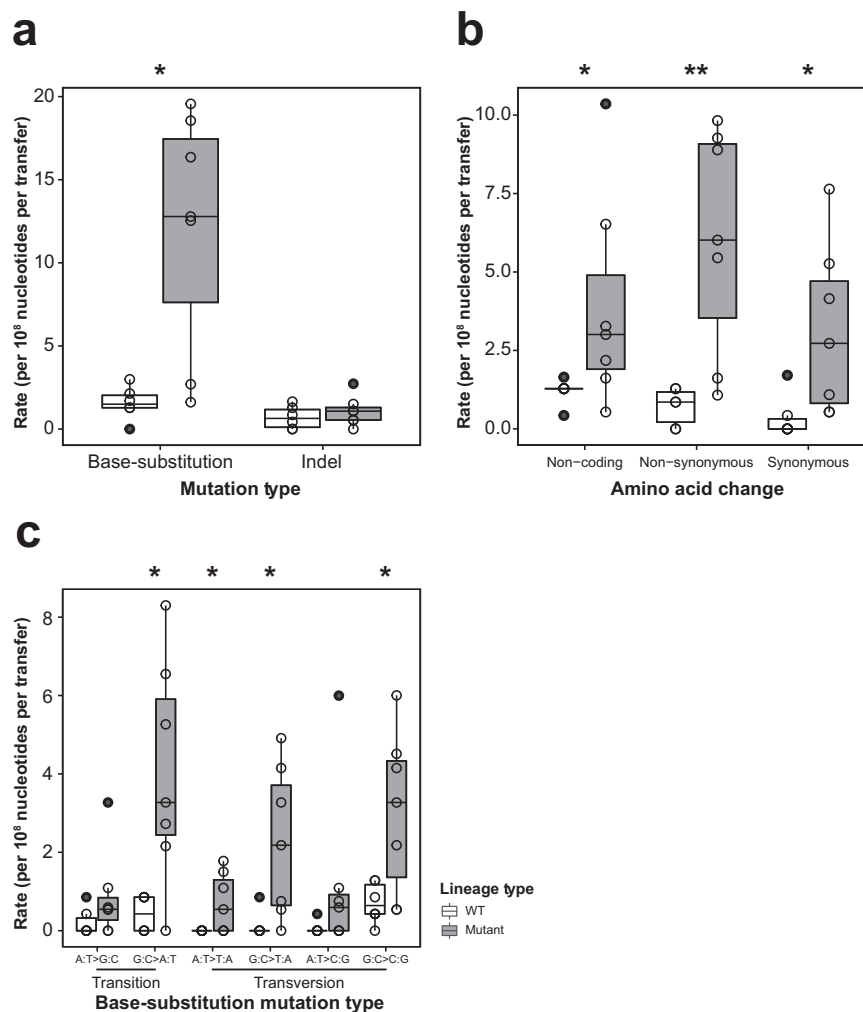


Fig. 5 Mutation rates of WT and mutant lineages for different mutation classes. Mutation rates are partitioned according to: **a** base-substitutions and indels; **b** the types of amino acid changes; and **c** for different classes of transitions or transversions. Mutation rates are calculated from $n = 6$ WT lineages or $n = 7$ mutant lineages. Box plots indicate median (middle line), 25th, 75th percentile (box), minimum, maximum (whiskers), and outliers (black points) as well as individual data points (open circles). Levels of statistical significance are indicated as $*P < 0.05$ and $**P < 0.01$ (Wilcoxon rank sum test).

reductions, either alone or in combination. In addition to genome loss, we were surprised that mutant lineages, but not WT ones, have an approximately 10-fold increased mutation rate, likely due to mutations in genes for DNA replication and repair^{19,20}. Mutations were found in several mutation classes and are higher in both coding and non-coding regions, indicating broad and non-specific mutagenesis. Decreased competitiveness, the massively compromised CFU as cells pass through single spore bottlenecks, and the combined accumulation of large deletions and an increased mutation burden, lead to synergistic declines in fitness that resembles a type of mutational meltdown. First, ecologically deficient mutants develop a higher mutation rate. Second, these lineages accumulate further deletions, which magnifies their fitness reductions and causes an irreversible decrease in their effective population size, ultimately leading to extinction. Although this process occurs within an organism over a very short time period, it closely resembles the idea of a classical mutational meltdown, in which a small population going through Muller's ratchet experiences accelerating fitness declines caused by deleterious mutations³⁸.

Even though mutant lineages are deteriorating at a pace that exceeds results from other MA experiments, they don't die immediately, as do *E. coli* colicin producers. Why do antibiotic

producing strains of *Streptomyces* die via mutational meltdown instead of lysing? One possible cause of this difference may be the intrinsic differences in the activity of antibiotics and colicins. Whereas the latter can act at very low concentrations, e.g., via single-hit kinetics³¹, antibiotics may require higher concentrations to provide sufficient protection to large *Streptomyces* colonies. Antibiotics can also bind tightly to abiotic substrates, potentially requiring higher levels of production within colonies³⁹. These possibilities would necessitate continued survival and growth of producing cells, thereby generating spatially clustered mutant subpopulations within colonies that hyperproduce antibiotics, whereas sufficient toxin quantities could be produced by single *E. coli* cells either dispersed randomly throughout the colony or on the colony edge facing impending threats^{32,33}. A related issue that remains unresolved is the origin of mutant cells within growing colonies, if they arise stochastically, are developmentally regulated, if mutants and the fraction of cells that adopt this fate are induced by local conditions in the soil environment, or some combination of these possibilities. Evidence suggests that the mutant fraction is at least partly environmentally dependent and can be modified by nutrients and other factors, including competition between strains. Competition with other species may also modify the degree to which this

division of labor benefits *S. coelicolor* colonies, including overall spore production. At the same time, there is undoubtedly a stochastic element because different colonies produce different mutants with different antibiotic production phenotypes. At present, we are unable to fully address these issues and they remain important areas for future work.

Altruistic behaviors can be explained by their indirect fitness benefits, whereby individuals offset the loss of their own reproduction by increasing the reproduction of their relatives⁴⁰. In multicellular bacteria, like streptomycetes or cyanobacteria, clonality, and therefore high relatedness, among cells in the colony is ensured by their mode of filamentous growth^{9,10}. For this reason, division of labor with extreme specialization can evolve and lead to the elaboration of multiple cell types. Streptomycetes are typically divided into two functional classes of cells: spores and vegetative cells^{11,12}. Our work supports the notion that colonies can be further partitioned into at least one more cell type, those producing antibiotics and that accumulate extreme and irreversible genetic damage leading to their demise. We would predict similar diversification among other streptomycetes, as well as the discovery of additional types of division of labor among other multicellular bacteria⁹.

Methods

Bacterial strains and cultural conditions. Strains used in this study are all derived from *Streptomyces coelicolor* A3 (2) M145. Strains were maintained and assayed at 30 °C on soy flour mannitol media (SFM) containing 20 g mannitol, 20 g agar, and 20 g soya flour per liter of water. Spores of *S. coelicolor* were diluted and plated onto an SFM plate. To obtain initial isolates for the MA experiment, one random WT colony (designated as WT_{ancestor}) was diluted and plated onto SFM plates. One random WT and mutant colony were then picked and replated onto separate SFM plates. Six random colonies were then chosen from each plate and designated as ancestors for subsequent serial passage through single colony transfer, for a total of 12 lineages (six WT and six mutants). During each transfer, a single colony from each lineage growing closest to a randomly placed spot on the back of the plate was chosen and streaked onto another SFM plate. This procedure was repeated every 3–4 days for 25 transfer cycles (Fig. 1b). Transferred lineages were archived by creating a full lawn from the transferred colony, after which spores were harvested after ~7 days of growth and sporulation as previously described⁴¹. All stocks were maintained at –20 °C.

Competition assay. We estimated the relative fitness of mutant (M1, M3, M4, M5, and M6) and WT lineages (W1–6) from T0 and T25 ($n = 2$ biologically independent replicates per WT strain and $n = 4$ biologically independent replicates per mutant strain), following the protocol in Zhang et al. (2020)¹³. All strains were marked with apramycin resistance and the WT ancestor was marked with hygromycin B resistance, by using integrating plasmids pSET152 and pIJ82, respectively. After diluting strains to 10^6 CFU ml⁻¹, they were mixed with the reciprocally marked WT ancestor at different initial frequencies. 100 µl of each mixture was plated onto 25 ml SFM agar plates and incubated at 30 °C for 5 days. At the same time, each mixture was serially diluted and plated onto SFM plates containing either apramycin (50 µg ml⁻¹) or hygromycin B (50 µg ml⁻¹) to obtain precise estimates of initial frequencies. After 5 days, each plate was harvested in Milli-Q H₂O and passed through an 18-gauge syringe plugged with cotton wool to remove mycelial fragments and resuspended in 1 ml 20% glycerol. Each sample was then serially diluted onto plates containing either antibiotic to calculate final frequencies.

Estimating antibiotic resistance. To estimate changes to antibiotic resistance, the MIC was determined for all strains by spotting dilution onto large SFM plates (150 × 20 mm, Sarstedt, Germany) supplemented with different antibiotic concentrations. Drug concentrations ranged from 2 to 32 µg ml⁻¹ (chloramphenicol, oxytetracycline, and ciprofloxacin) and 1 to 16 µg ml⁻¹ (streptomycin). Plates were inoculated using a 96-pin replicator from master 96-well plates containing ~ 10^7 spores ml⁻¹. Approximately 1 µl from this stock was applied to each plate; the replicator was flame sterilized between each transfer to ensure that no cells or antibiotics were transferred between assay plates. The plates were incubated for 4 days at 30 °C and then imaged and scored for growth. The MIC was determined as the drug concentration where no growth was visible after 4 days ($n = 3$ biologically independent replicates per strain per drug concentration).

Auxotrophy assay. To test for auxotrophy, strains were grown on minimal media (MM) containing per liter 0.5 g asparagine, 0.5 g K₂HPO₄, 0.2 g MgSO₄·7H₂O, 0.01 g FeSO₄·H₂O and 10 g agar, supplied with either 0.5% mannitol or 0.5%

mannitol plus 0.0079% arginine. Bacteria were spotted onto plates using a pin replicator, as for MIC assays, and grown for 4 days at 30 °C. Auxotrophy was detected by comparing the growth of colonies on plates with or without supplemented arginine ($n = 3$ biologically independent replicates per strain).

CFU estimation. We used CFU to estimate the fitness of strains from each lineage ($n = 3$ biologically independent replicates per strain except $n = 2$ for M1 from T19). For each strain, 10^5 spores were plated onto SFM as a confluent lawn. After 5 days of growth, spores were harvested by adding 10 ml Milli-Q H₂O to the plates, gently scraping the plate surface to create a spore suspension, and then filtering the liquid through an 18-gauge syringe with cotton wool to remove mycelia. After centrifugation, spore stocks were resuspended in 1 ml 20% glycerol and then serially diluted onto SFM to calculate the total CFU for each strain.

Estimating antibiotic production. All mutant (except M2) and WT lineages from T0 and T25 were tested for antibiotic production by measuring the zone of inhibition in an overlay assay. Spores were diluted to get 10^6 spores ml⁻¹ and subsequently 2 µl was spotted onto an SFM plate in the center. Three replicates of each strain were prepared and incubated for 5 days at 30 °C. On the 6th day, exponentially growing cultures of *B. subtilis* were prepared by subculturing an overnight grown strain in LB medium and incubated until the optical density at 600 nm (OD₆₀₀) 0.4–0.6 was achieved. Soft agar was prepared by mixing LB liquid with LB agar in a 1:1 ratio and maintained at 60 °C. 150 µl of the exponentially growing *B. subtilis* was added to 7 ml of soft agar, mixed adequately, and poured onto the SFM plate containing the *Streptomyces* spot growing in the center. The soft agar was allowed to solidify and the plates were subsequently incubated overnight at 30 °C. The plates were scanned the next day and the area of inhibition/clearance was measured using the ImageJ/Fiji software (v 1.53c)⁴².

Whole-genome sequencing. Sequenced strains include WT_{ancestor}, M1–M6 from T0, W3 from T5, W3 from T7, and all lineages from T25. Strains were sequenced using two approaches. Long reads sequencing (PacBio, USA) was performed as previously reported¹³. Short reads sequencing (BGISEQ-500) was done using the following protocol. DNA was extracted after growth in liquid TSBS: YEME (1:1 v:v) supplemented with 0.5% glycine and 5 mM MgCl₂. Approximately 10^8 spores were inoculated in 25 ml and incubated at 30 °C with a shaking speed of 200 rpm for 12–48 h. TSBS contains 30 g tryptic soya broth powder and 100 g sucrose per liter and YEME contains 3 g yeast extract, 5 g peptone, 3 g malt extract, 10 g glucose and 340 g sucrose per liter. DNA was extracted using phenol/chloroform⁴¹. Visible cell pellets were washed with 10.3% sucrose solution after centrifugation. Pellets were resuspended in 300 µl GTE buffer, containing 50 mM glucose, 10 mM EDTA, 20 mM Tris-HCl, pH 7.5 and 4 mg ml⁻¹ lysozyme and incubated at 37 °C for 1 h. Then 300 µl 2 M NaCl was added and gently inverted ten times, followed by the addition of 500 µl phenol/chloroform (bottom layer). After mixing, each tube was centrifuged for 5 min and the upper layer was transferred to a new tube. This procedure was repeated at least twice until the intermediate layer was almost invisible. The final transferred upper layer was mixed with a same volume of 2-propanol, and centrifugated for 10 min. Liquid in the supernatant was discarded and pellets were dried at room temperature before being dissolved in 200 µl Milli-Q H₂O. After adding 1 µl RNase, the DNA was resuspended at 37 °C for 1 h. Phenol/chloroform washing and DNA precipitation was repeated once to remove the RNase. After adding phenol/chloroform, the upper layer was transferred to a new tube, and then mixed with 16 µl 3 M pH 5.2 NaCH₃COO and 400 µl 96% ethanol. This mixture was cooled at –20 °C for 1 h and centrifuged for 10 min to obtain the DNA pellets. Pellets were washed with pre-cooled 96% ethanol and dried at room temperature. DNA was dissolved in Milli-Q H₂O and sent for commercial sequencing at BGI (Hong Kong).

Sequence data processing. The raw data of PacBio sequencing were processed as outlined in Zhang et al. (2020)¹³ by using BLASR (v 5.3.2)⁴³, SAMtools (v 1.9)⁴⁴, and IGV (v 2.4.15)^{45,46}. Genome length was evaluated based on these results. The BGISEQ-500 data were handled using CLC Genomics Workbench (QIAGEN, v 8.5.4). Filtered raw reads were first imported and mapped to the reference genome NC_003888.3⁴⁷ through the “NGS core” - “Map to the reference” function. Variants were then called by using “Basic variant detection” function, with the filter parameters set to minimum coverage as 5, minimum count as 2, and minimum frequency as 50%. Variants were identified by comparing lineages to their corresponding parental strain by applying the “Resequencing analysis” - “Compare Variants” - “Compare Sample Variant Tracks” option. By using the annotation information in the GenBank file, final variants were then annotated by applying the “Track tools” - “Annotate with overlap information” option, and amino acid changes were added to the variant track by “Resequencing analysis” - “Functional consequences” - “Amino acid changes” option. Final results were exported as excel sheets and variants in genes that were not detected in PacBio sequencing were removed before performing further analyses.

Statistical analyses. All statistical analyses were performed in R (v 3.6.2). Shapiro–Wilk test was used to check the normality of data. Welch’s *t* test was used to test differences in CFU production, relative fitness and antibiotic production

across the course of the experiment. Specifically, one-sided one-sample *t* test was used to compare the antibiotic production of W3. One-sample Wilcoxon signed rank test was used to test if the CFU changed after transfers while Wilcoxon rank sum test was used to compare the difference between WT and mutant lineages. Unless specified, all tests are two-sided. Pearson's product-moment correlation was performed to indicate the correlation between CFU production and relative fitness or the deletion size.

Reporting summary. Further information on research design is available in the Nature Research Reporting Summary linked to this article.

Data availability

Raw sequencing data that support the findings of this study have been deposited in NCBI's Sequence Read Archive (SRA) database via a BioProject with accession number PRJNA780771. Source data are provided with this paper.

Received: 13 November 2020; Accepted: 8 April 2022;

Published online: 27 April 2022

References

- Fisher, R. M., Cornwallis, C. K. & West, S. A. Group formation, relatedness, and the evolution of multicellularity. *Curr. Biol.* **23**, 1120–1125 (2013).
- Queller, D. C. Relatedness and the fraternal major transitions. *Philos. Trans. R. Soc. B Biol. Sci.* **355**, 1647–1655 (2000).
- West, S. A. & Cooper, G. A. Division of labour in microorganisms: an evolutionary perspective. *Nat. Rev. Microbiol.* **14**, 716–723 (2016).
- Cooper, G. A. & West, S. A. Division of labour and the evolution of extreme specialization. *Nat. Ecol. Evol.* **2**, 1161–1167 (2018).
- Gilbert, O. M., Foster, K. R., Mehdiabadi, N. J., Strassmann, J. E., & Queller, D. C. High relatedness maintains multicellular cooperation in a social amoeba by controlling cheater mutants. *Proc. Natl Acad. Sci. U. S. A.* **104**, 8913–8917 (2007).
- Kuzdzal-Fick, J. J., Fox, S. A., Strassmann, J. E. & Queller, D. C. High relatedness is necessary and sufficient to maintain multicellularity in *Dictyostelium*. *Science* **334**, 1548–1551 (2011).
- Velicer, G. J. & Vos, M. Sociobiology of the myxobacteria. *Annu. Rev. Microbiol.* **63**, 599–623 (2009).
- Queller, D. C. & Strassmann, J. E. Kin selection and social insects: social insects provide the most surprising predictions and satisfying tests of kin selection. *Bioscience* **48**, 165–175 (1998).
- Claessen, D., Rozen, D. E., Kuipers, O. P., Søgaard-Andersen, L. & van Wezel, G. P. Bacterial solutions to multicellularity: a tale of biofilms, filaments and fruiting bodies. *Nat. Rev. Microbiol.* **12**, 115–124 (2014).
- Zhang, Z., Claessen, D. & Rozen, D. E. Understanding microbial divisions of labor. *Front. Microbiol.* **7**, 2070 (2016).
- Chater, K. F. & Losick, R. The mycelial life-style of *Streptomyces coelicolor* A3(2) and its relatives. In *Bacteria as multicellular organisms* 149–182 (Oxford University Press, 1997).
- Flårdh, K. & Buttner, M. J. *Streptomyces* morphogenetics: dissecting differentiation in a filamentous bacterium. *Nat. Rev. Microbiol.* **7**, 36–49 (2009).
- Zhang, Z. et al. Antibiotic production in *Streptomyces* is organized by a division of labor through terminal genomic differentiation. *Sci. Adv.* **6**, eaay5781 (2020).
- Barka, E. A. et al. Taxonomy, physiology, and natural products of Actinobacteria. *Microbiol. Mol. Biol. Rev.* **80**, 1–43 (2016).
- van der Heul, H. U., Bilyk, B. L., McDowall, K. J., Seipke, R. F. & van Wezel, G. P. Regulation of antibiotic production in Actinobacteria: new perspectives from the post-genomic era. *Nat. Prod. Rep.* **35**, 575–604 (2018).
- Lynch, M. et al. Genetic drift, selection and the evolution of the mutation rate. *Nat. Rev. Genet.* **17**, 704–714 (2016).
- Andersson, D. I. & Hughes, D. Muller's ratchet decreases fitness of a DNA-based microbe. *Proc. Natl Acad. Sci. U. S. A.* **93**, 906–907 (1996).
- Kibota, T. T. & Lynch, M. Estimate of the genomic mutation rate deleterious to overall fitness in *E. coli*. *Nature* **381**, 694–696 (1996).
- Horst, J. P., Wu, T. & Marinus, M. G. *Escherichia coli* mutator genes. *Trends Microbiol.* **7**, 29–36 (1999).
- Liu, V. F., Bhaumik, D. & Wang, T. S.-F. Mutator phenotype induced by aberrant replication. *Mol. Cell. Biol.* **19**, 1126–1135 (1999).
- Flett, F. & Cullum, J. DNA deletions in spontaneous chloramphenicol-sensitive mutants of *Streptomyces coelicolor* A3(2) and *Streptomyces lividans* 66. *MGG Mol. Gen. Genet.* **207**, 499–502 (1987).
- Vecchione, J. J., Alexander, B. & Sello, J. K. Two distinct major facilitator superfamily drug efflux pumps mediate chloramphenicol resistance in *Streptomyces coelicolor*. *Antimicrob. Agents Chemother.* **53**, 4673–4677 (2009).
- Flett, F., Platt, J. & Cullum, J. DNA rearrangements associated with instability of an arginine gene in *Streptomyces coelicolor* A3(2). *J. Basic Microbiol.* **27**, 3–10 (1987).
- Claessen, D., de Jong, W., Dijkhuizen, L. & Wösten, H. A. B. Regulation of *Streptomyces* development: reach for the sky! *Trends Microbiol.* **14**, 313–319 (2006).
- van Gestel, J., Vlamakis, H. & Kolter, R. Division of labor in biofilms: the ecology of cell differentiation. *Microbiol. Spectr.* **3**, MB-0002-2014 (2015).
- Giri, S., Waschina, S., Kaleta, C. & Kost, C. Defining division of labor in microbial communities. *J. Mol. Biol.* **431**, 4712–4731 (2019).
- Dragoś, A. et al. Division of labor during biofilm matrix production. *Curr. Biol.* **28**, 1903–1913 (2018).
- Geerlings, N. M. J. et al. Division of labor and growth during electrical cooperation in multicellular cable bacteria. *Proc. Natl Acad. Sci. U. S. A.* **117**, 5478–5485 (2020).
- Herrero, A., Stavans, J. & Flores, E. The multicellular nature of filamentous heterocyst-forming cyanobacteria. *FEMS Microbiol. Rev.* **40**, 831–854 (2016).
- von Bronk, B., Schaffer, S. A., Götz, A. & Opitz, M. Effects of stochasticity and division of labor in toxin production on two-strain bacterial competition in *Escherichia coli*. *PLoS Biol.* **15**, e2001457 (2017).
- Cascales, E. et al. Colicin biology. *Microbiol. Mol. Biol. Rev.* **71**, 158–229 (2007).
- Mavridou, D. A. I., Gonzalez, D., Kim, W., West, S. A. & Foster, K. R. Bacteria use collective behavior to generate diverse combat strategies. *Curr. Biol.* **28**, 345–355 (2018).
- Granato, E. T. & Foster, K. R. The evolution of mass cell suicide in bacterial warfare. *Curr. Biol.* **30**, 2836–2843 (2020).
- Robinson, G. E. Regulation of division of labor in insect societies. *Annu. Rev. Entomol.* **37**, 637–665 (1992).
- Muller, H. J. The relation of recombination to mutational advance. *Mutat. Res. - Fundam. Mol. Mech. Mutagen* **1**, 2–9 (1964).
- Felsenstein, J. The evolution advantage of recombination. *Genetics* **78**, 737–756 (1974).
- Kurokawa, M., Seno, S., Matsuda, H. & Ying, B. W. Correlation between genome reduction and bacterial growth. *DNA Res* **23**, 517–525 (2016).
- Gabriel, W., Lynch, M. & Burger, R. Muller's ratchet and mutational meltdowns. *Evolution* **47**, 1744–1757 (1993).
- Cycoń, M., Mrozik, A. & Piotrowska-Seget, Z. Antibiotics in the soil environment—degradation and their impact on microbial activity and diversity. *Front. Microbiol.* **10**, 338 (2019).
- West, S. A., Griffin, A. S. & Gardner, A. Evolutionary explanations for cooperation. *Curr. Biol.* **17**, R661–R672 (2007).
- Kieser, T. et al. *Practical Streptomyces genetics*. (John Innes Foundation, 2000).
- Schindelin, J. et al. Fiji: an open-source platform for biological-image analysis. *Nat. Methods* **9**, 676–682 (2012).
- Chaisson, M. J. & Tesler, G. Mapping single molecule sequencing reads using basic local alignment with successive refinement (BLASR): application and theory. *BMC Bioinforma.* **13**, 238 (2012).
- Danecek, P. et al. Twelve years of SAMtools and BCFtools. *Gigascience* **10**, 1–4 (2021).
- Robinson, J. T. et al. Integrative genomics viewer. *Nat. Biotechnol.* **29**, 24–26 (2011).
- Thorvaldsdóttir, H., Robinson, J. T. & Mesirov, J. P. Integrative genomics viewer (IGV): High-performance genomics data visualization and exploration. *Brief. Bioinform.* **14**, 178–192 (2013).
- Bentley, S. D. et al. Complete genome sequence of the model actinomycete *Streptomyces coelicolor* A3(2). *Nature* **417**, 141–147 (2002).

Acknowledgements

Z.Z. was supported by China Scholarship Council (CSC). S.S. was supported by a NWA startimpulse grant from Origins Center. D.C. was funded by a Vici grant (Grant number VI.C.192.002) from the Dutch Research Council (NWO). We would like to thank Chao Du for his help with bioinformatics and data visualization.

Author contributions

Z.Z., D.C., and D.E.R. conceptualized this study. Z.Z., S.S., and B.C. performed the experimental work. Z.Z., S.S., D.C., and D.E.R. analyzed the results. Z.Z., S.S., D.C., and D.E.R. wrote the manuscript. All authors approved the final submitted version of this paper.

Competing interests

The authors declare no competing interests.

Additional information

Supplementary information The online version contains supplementary material available at <https://doi.org/10.1038/s41467-022-29924-y>.

Correspondence and requests for materials should be addressed to Zheren Zhang or Daniel E. Rozen.

Peer review information *Nature Communications* thanks the other anonymous reviewer(s) for their contribution to the peer review of this work.

Reprints and permission information is available at <http://www.nature.com/reprints>

Publisher's note Springer Nature remains neutral with regard to jurisdictional claims in published maps and institutional affiliations.



Open Access This article is licensed under a Creative Commons Attribution 4.0 International License, which permits use, sharing, adaptation, distribution and reproduction in any medium or format, as long as you give appropriate credit to the original author(s) and the source, provide a link to the Creative Commons license, and indicate if changes were made. The images or other third party material in this article are included in the article's Creative Commons license, unless indicated otherwise in a credit line to the material. If material is not included in the article's Creative Commons license and your intended use is not permitted by statutory regulation or exceeds the permitted use, you will need to obtain permission directly from the copyright holder. To view a copy of this license, visit <http://creativecommons.org/licenses/by/4.0/>.

© The Author(s) 2022